Cooperative Resource Scheduling for Environment Sensing in Satellite–Terrestrial Vehicular Networks

Mingcheng He, *Graduate Student Member, IEEE*, Huaqing Wu, *Member, IEEE*, Xuemin Shen, *Fellow, IEEE*, and Weihua Zhuang, *Fellow, IEEE*

***Abstract*—In this article, we investigate infrastructure-assisted environment sensing in satellite-terrestrial vehicular networks (STVN) for connected autonomous vehicles (CAVs), where satellites and roadside units (RSUs) cooperate to provide CAVs with fresh sensing data. To support satellite- and RSU-assisted environment sensing for CAVs, we formulate a long-term resource scheduling problem in STVN to satisfy sensing data freshness requirements with efficient resource usage. To deal with the challenges posed by the dynamic network environment as well as stringent data freshness requirements, we propose a cooperative satellite-terrestrial resource scheduling (CSTRS) scheme. CSTRS is a model-data co-driven approach that can jointly optimize the sensing interval and resource allocation in STVN. Specifically, benefiting from the multicast feature of the low Earth orbit satellite, coalition game, and particle swarm optimization-based algorithms are designed to partition CAVs into groups and optimize sensing intervals in large timescales. Then, a reinforcement learning-based algorithm is developed to make real-time computing and communication resource allocation decisions based on the CAV partition. Simulation results demonstrate that the proposed scheme outperforms benchmark methods in terms of resource usage and reliability performance.**

***Index Terms*—Coalition game, cooperative resource scheduling, reinforcement learning, satellite-terrestrial vehicular networks (STVNs).**

I. Introduction

As THE number of connected autonomous vehicles (CAVs) on the road increases tremendously, the acquisition of real-time environment data becomes imperative for optimizing driving routes and enhancing the overall travel experience [1]. Specifically, each CAV needs surrounding environment information within its Range of Interest (RoI), for improving transportation safety and efficiency. With the help of the built-in processors of CAVs, onboard sensors are able to sense the surrounding environment and process the sensing data to detect objects, such as nonconnected vehicles, obstacles, etc. However, considering the limited sensing area as well as the potential blockage from a single CAV view, augmenting the sensing range and mitigating blocked areas are essential. Infrastructure-assisted environment sensing, using sensors deployed on different network infrastructures, can provide large-range traffic information within the RoI of CAVs to increase the trust level of the observation [2]. To maintain up-to-date environment information in CAVs, freshness and reliability of sensing results are crucial to avoid data expiration. However, the freshness of sensing results diminishes over time, underscoring the importance of maintaining a high freshness level for high safety and optimal CAV control.

Currently, most sensors, including cameras and LIDAR sensors are deployed on terrestrial infrastructure, such as roadside units (RSUs) to support environment sensing [3]. By deploying edge servers on RSUs, the sensing data, such as images of the covered area, can be processed to generate sensing results. These results are then transmitted to CAVs within the RSUs' service range to update surrounding traffic information. The significant computing and communication capabilities of RSUs for data processing and transmission enable environment sensing with low latency and high reliability, making terrestrial networks the primary choice for serving CAVs. However, RSUs face limitations in global deployment due to high costs and geographical constraints, especially in rural or remote areas. This can lead to a lack of sensing services or outdated sensing data over time.

To enlarge the network coverage to support CAVs, low Earth orbit (LEO) satellites offer a promising solution [4], [5]. With their dense deployment and ubiquitous coverage, LEO satellites can effectively complement terrestrial vehicular networks to provide seamless network services. Remote sensing LEO satellites have been studied for many years, where high-resolution satellite images allow the monitoring of road traffic conditions to improve traffic efficiency [6]. With edge computing capabilities equipped on LEO satellites, the sensing data can be processed directly, eliminating the need to transmit large volumes of raw data to ground servers and reducing transmission delay. Nevertheless, satellites have high velocities and resource costs compared to terrestrial networks. To take full advantage of the complementary strengths of satellites and RSUs for environment sensing while satisfying the freshness requirement and optimizing resource utilization, cooperative resource scheduling from both satellite and terrestrial networks in satellite-terrestrial vehicular networks (STVNs) is critical.

Significant research efforts have been put into cooperative resource scheduling in satellite-terrestrial integrated

Received 18 July 2024; revised 16 October 2024; accepted 29 October 2024. Date of publication 7 November 2024; date of current version 7 March 2025. This work was supported by the Natural Sciences and Engineering Research Council of Canada (NSERC) under Grant RGPIN-2023-03759. *(Corresponding author: Mingcheng He.)*

Mingcheng He, Xuemin Shen, and Weihua Zhuang are with the Department of Electrical and Computer Engineering, University of Waterloo, Waterloo, ON N2L 3G1, Canada (e-mail: mingcheng.he@uwaterloo.ca; sshen@uwaterloo.ca; wzhuang@uwaterloo.ca).

Huaqing Wu is with the Department of Electrical and Software Engineering, University of Calgary, Calgary, AB T2N 1N4, Canada (e-mail: huaqing.wu1@ucalgary.ca).

Digital Object Identifier 10.1109/JIOT.2024.3493613

networks (STINs) to jointly manage resources from both satellite and terrestrial components. A cooperative multigroup multicast transmission scheme is proposed in [7], where the pregrouping is applied to improve the spectrum efficiency in satellite multicast transmission. A joint association and bandwidth allocation scheme is proposed in [8] in STVN to reduce the system cost while satisfying service quality requirements. Zhou et al. [9] investigated a learning-based algorithm for access mode selection in STVN with enhanced network flexibility and reliability by exploiting the advantages of different networks to support vehicular services.

Despite these research endeavors, cooperative resource scheduling for both satellite and terrestrial networks still encounters several challenges in supporting environment sensing. First, to maintain the freshness of sensing results in each CAV, two factors need to be jointly considered: 1) sensing interval and 2) infrastructure-related delays in data processing and result transmission, which leads to a highly complex resource scheduling strategy in a dynamic network environment. Second, the mobility of LEO satellites and CAVs results in varying distances between them over time, introducing fluctuations in propagation delay, communication performance, and network accessibility. This variability leads to changing resource demands from both satellite and terrestrial networks. Third, LEO satellites and RSUs in STVN have heterogeneous network features in terms of coverage areas and content delivery modes. Due to the distinct coverage areas of satellites and RSUs, connection durations for CAVs differ between satellite and terrestrial components. Meanwhile, each network component needs to schedule both computing and communication resources with varying resource costs for environment sensing. This makes the cooperative resource scheduling between satellite and terrestrial networks complicated. It requires managing varying connectivity patterns and resource differentiations, involving multiple decisions to ensure seamless service and data freshness for CAVs.

To address the above mentioned challenges, we propose a cooperative satellite-terrestrial resource scheduling (CSTRS) scheme in this article. CSTRS scheme aims to cooperatively allocate communication and computing resources as well as determine sensing intervals in STVN, ensuring stringent data freshness requirements with efficient resource utilization. Specifically, a hybrid data-model co-driven approach is developed to find the optimal solutions in two steps for simplifying the decision making. Leveraging the multicast feature of LEO satellites to serve a group of CAVs simultaneously with less resource consumption, we design model-based sensing interval determination and CAV partitioning methods in a large timescale for reducing the computing and communication resource cost and the resource allocation complexity. Based on the CAV grouping and sensing interval, a reinforcement learning-based algorithm is then developed for the real-time computing and communication resource allocation decisions for different CAV groups to cope with time-varying network dynamics. The main contributions of this article are summarized as follows.

TABLE I
LIST OF ACRONYMS

Acronym	Term
AoI	Age of Information
CAV	Connected Autonomous Vehicle
LEO	Low Earth Orbit
MDP	Markov Decision Process
PPO	Proximal Policy Optimization
PSO	Particle Swarm Optimization
RoI	Range of Interest
RSU	Roadside Unit
STVN	Satellite-Terrestrial Vehicular Networks
TSG/SSG	Terrestrial/Satellite Service Group

1) We investigate the resource scheduling problem in STVN to support infrastructure-assisted environment sensing for CAVs, where both LEO satellites in satellite networks and RSUs in terrestrial networks can provide network services for CAVs. Specifically, we formulate the cooperative resource scheduling problem for allocating computing and communication resources as well as determining sensing interval and CAV partitioning to satisfy the data freshness requirements with efficient resource consumption.
2) We propose the CSTRS scheme to solve the mixed-integer sequential decision-making resource scheduling problem. In this scheme, the original problem is decoupled into two subproblems to reduce the complexity. Specifically, CAV partition and sensing interval decisions are adjusted in a large timescale, while resource allocation for each service group (SG) is determined in a small timescale.
3) We design a particle swarm optimization (PSO)-based algorithm to optimize the long-term sensing interval and a coalition formation game-based approach to determine CAV partition, with reduced resource cost and decision-making complexity. The real-time communication and computing resource allocation subproblem is solved by the proposed proximal policy optimization (PPO)-based reinforcement learning algorithm to cope with dynamic environments.

The remainder of this article is organized as follows. In Section II, we provide a comprehensive review of resource scheduling studies in STVN. The considered network scenario and system models are given in Section III. The problem formulation and decoupling are presented in Section IV. Then, a two-step CSTRS scheme is proposed, where a PSO-based optimization algorithm and a coalition formation game are designed for determining sensing interval and CAV partitioning for long-term decisions in Section V, and a reinforcement learning-based algorithm for real-time computing and communication resource allocation is provided in Section VI. Performance evaluation is given in Section VII to demonstrate the performance of the proposed scheme, followed by the conclusions in Section VIII. A list of acronyms used in this article is shown in Table I.

II. Related Work

STINs are envisioned as a promising architecture to complement terrestrial networks to realize seamless and ubiquitous network coverage. In the literature, there exist a few works investigating resource scheduling in STIN to support different services. Zhu et al. [7] proposed a cooperative multigroup multicast transmission scheme in STIN where the pregrouping is applied for different users with different required content. Beamforming adjustment of the terrestrial base station and the satellite is also investigated to maximize the minimum SINR among all users. A cooperative resource management algorithm is proposed in [10] where satellite networks and terrestrial networks support the access of massive Internet of Things (IoT) devices by sharing the same spectrum resource. An intelligent spectrum management framework for the STIN is designed in [11] to transform heterogeneous networks into integrated networks with interoperability for two networks and provide cooperative management for the STIN through a centralized controller. In [12], a nonorthogonal multiple access-based Age of Information (AoI) minimization is investigated in STIN by selecting base station-terrestrial user pairs and optimizing transmit power. An auction-based relay node selection algorithm is proposed in [13] for IoT nodes in the STIN to maximize the sum transmission rate, considering that the satellite networks have extensive coverage and can alleviate the spectrum scarcity of terrestrial networks.

In addition, leveraging the computing or caching capability in satellites and terrestrial base stations, several works study the cooperative scheduling among different resources in STIN. In [14], a learning-based joint cache placement and content delivery algorithm is proposed to minimize the long-term overall transmission delay by providing a long-term decision of cache placement and a short-term decision of user association with either satellites or terrestrial base stations. A cost-effective hybrid computation offloading paradigm in STIN is proposed in [15], which aims to minimize total computation offloading costs while satisfying diverse user latency requirements and adhering to satellite energy constraints, while a hybrid PPO-based algorithm to support task offloading in STIN for remote IoT users is developed in [16] for minimizing offloading delay.

There have also been several works supporting diversified vehicular applications in STVN. In [5], network performance is analyzed in different scenarios in STVN with different satellite constellation settings and terrestrial network deployments. A resource slicing and scheduling problem of STVN supporting delay-sensitive and delay-tolerant service is studied in [8] to satisfy service quality requirements with minimum system cost. By jointly considering mobility patterns and fluctuating loads in STVN, a time-varying resource graph is proposed in [17] to model dynamic resources for better resource allocation. While several research works study the resource scheduling in STVN, supporting infrastructure-assisted environment sensing is still an open problem considering the cooperative resource allocation and sensing interval determination from satellite and terrestrial networks to meet stringent data freshness requirements. Therefore, in this article, we propose a CSTRS scheme to satisfy freshness requirements with efficient resource usage in STVN.

TABLE II
Summary of Notations

Notation	Definition
$\mathbf{p}^{\mathrm{S}}, \mathbf{p}_n^{\mathrm{T}}, \mathbf{p}_{\mathbf{s}}^{\mathrm{SSG}}$	Coordination of the LEO satellite, RSU n, and the center of SSG $\mathbf{s}$
$a_u^{\mathrm{T}}(t)$	RSU accessibility for CAV u at time slot t
$\Omega^{\mathrm{S}}(t), \Omega^{\mathrm{T}}(t)$	Set of SSGs and TSGs at time slot t
$I_{\mathbf{g}}^{\mathrm{T}}(t)$, $I_{\mathbf{s}}^{\mathrm{S}}(t)$	Sensing intervals for SSG $\mathbf{s}$ and TSG $\mathbf{g}$
$\nu_{\mathbf{s}}^{\mathrm{S}}(t)$, $\beta_{\mathbf{s}}^{\mathrm{S}}(t)$	Sensing data size and sensing result data size for SSG $\mathbf{s}$
$Q_{\mathbf{s}}^{\mathrm{S}}(t)$, $W_{\mathbf{s}}^{\mathrm{S}}(t)$, $Z_{\mathbf{s}}^{\mathrm{S}}(t)$	Remaining processing data size, transmission data size, and propagation time for SSG $\mathbf{s}$
$c_{\mathbf{s}}^{\mathrm{S}}(t), b_{\mathbf{s}}^{\mathrm{S}}(t)$	Computing and communication resources allocated for SSG $\mathbf{s}$ at time slot t
$\chi_1^{\mathrm{S}}, \chi_2^{\mathrm{S}}, \chi_1^{\mathrm{T}}, \chi_2^{\mathrm{T}}$	Unit cost of computing and communication resource in the satellite and RSUs
T_u^{S}, T_u^{T}, $\hat{\psi}_u^{\mathrm{S}}$	Sensing interval from the satellite and RSUs, and offset set for CAV u
$q_u(t), q_{\mathbf{s}}^{\max}(t)$	Overall AoI for CAV u and maximum AoI value in SSG $\mathbf{s}$
$H_{\mathbf{s}}^{\max}(t)$	Maximal virtual reliability queue value of CAVs in SSG $\mathbf{s}$

III. Network Scenario and System Model

In this section, we first introduce the STVN scenario for infrastructure-assisted environment sensing and then describe the system models. Some useful notations are listed in Table II for easy reference.

A. Network Scenario

The infrastructure-assisted environment sensing for CAVs in the STVN is shown in Fig. 1. Specifically, terrestrial RSUs can support environment sensing for CAVs within their coverage areas. However, due to high deployment and maintenance costs or geographical constraints, RSUs can hardly guarantee full coverage, especially in remote areas. Therefore, LEO satellites can be utilized to complement terrestrial RSUs in supporting environment sensing. A central controller on the ground manages all RSUs and the LEO satellite covering the area. Here, we consider LEO satellites with steerable beams to cover the service area in a fixed time [18]. Consider a time-slotted system where each time slot $t \in \mathcal{T} = \{1, 2, \ldots, T\}$ has the same duration, denoted by τ, and T is the duration of LEO satellite service for a given area following the minimum elevation angle requirement. Let $(r^S, \alpha, \omega(t), \rho(t))$ illustrate the time-varying position of the LEO satellite at time slot t, where r^S is the LEO satellite orbit radius, α is the orbital inclination angle, $\omega(t)$ is the longitude of the ascending node of the orbit, and $\rho(t)$ is the argument of periapsis, defining the angle measured from the ascending node of the orbit to the satellite. The Cartesian coordination of the satellite at time slot t can therefore be transformed and given by $\mathbf{p}^S(t) = (x^S(t), y^S(t), z^S(t))$ according to [5]. Let $\mathcal{N} = \{1, 2, \ldots, N\}$ denote the set of RSUs serving the target area,

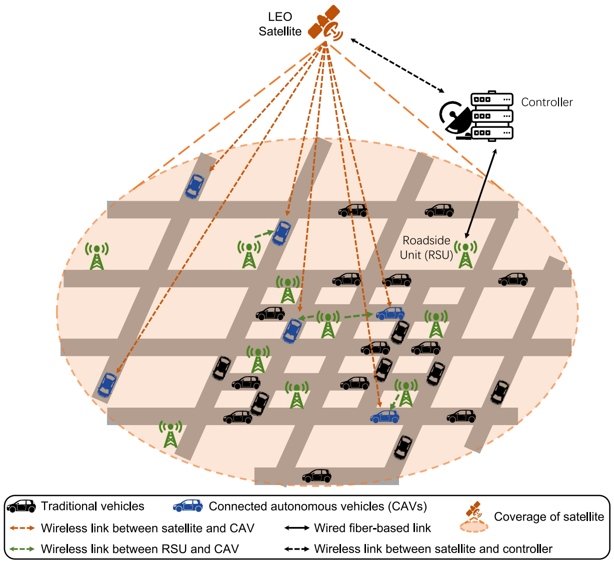

Fig. 1. Considered environment sensing scenario in STVN.

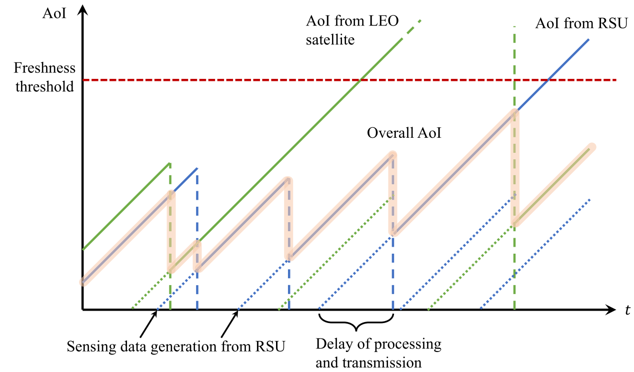

Fig. 2. AoI illustration of CAV.

where each RSU has a fixed coverage radius of r^T. The Cartesian coordinate of RSU n is $\mathbf{p}_n^T = (x_n^T, y_n^T, z_n^T)$. Let $\mathcal{U} = \{1, 2, \ldots, U\}$ denote the set of CAVs, where each CAV has the coordinate $\mathbf{p}_u^U(t) = (x_u^U(t), y_u^U(t), z_u^U(t))$ at time slot t. Considering the mobility of CAVs, the accessibility to RSUs and satellites may change over time. Let $a_u^T(t)$ represent the RSU accessibility for CAV u at time slot t. If $a_u^T(t) = 1$, CAV u can access at least one RSU at time slot t, while if $a_u^T(t) = 0$, CAV u cannot access to any RSU.

Consider that both LEO satellites and RSUs have the capability of data processing with the deployment of edge servers. For infrastructure-assisted environment sensing, the LEO satellite and RSUs need to periodically sense the RoI of CAVs, process the sensing data, and deliver the sensing results to CAVs. Processing and transmitting the sensing data related to the RoI of each individual CAV may lead to unnecessarily excessive consumption of computing and communication resources due to the potential overlaps among different CAVs' RoIs. To mitigate this issue, we leverage the multicast feature of LEO satellites to serve a bunch of CAVs simultaneously to enhance computing resource and bandwidth utilization. Specifically, we establish multiple satellite SGs (SSGs) for environment sensing from the satellite, where each group contains a subset of CAVs. Let $\Omega^S(t) = \{\mathbf{s}_0(t), \mathbf{s}_1(t), \ldots, \mathbf{s}_m(t)\}$ denote the SSGs, where $\mathbf{s}_i(t), i \neq 0$ is the ith SSGs served by the LEO satellite at time slot t and $\mathbf{s}_0(t)$ is the CAV group not served by the satellite. On the other hand, due to the small coverage of RSUs, we consider that each RSU serves one terrestrial SG (TSG) consisting of all CAVs within its coverage. Specifically, each RSU periodically senses the environment within its coverage, processes the sensing data, and transmits the result to all covering CAVs. In this case, TSGs can be denoted by $\Omega^T(t) = \{\mathbf{g}_1(t), \ldots, \mathbf{g}_n(t)\}$, where $\mathbf{g}_i(t)$ is the set of CAVs in the ith TSG served by RSU i. Considering the mobility of CAVs, CAVs in each TSG may change over time and SSGs are adjusted in a constant time interval, consisting of k time slots.

To satisfy the data freshness requirement, determining a proper sensing interval is essential for each SG. Basically, a small sensing interval enables tracking real-time vehicle behavior but leads to stringent processing and transmission delay requirements, consuming a large amount of resources. On the other hand, a large sensing interval may violate the freshness requirements. Considering that sensing from the satellite and RSUs can both affect the freshness of the sensing results, the sensing interval from different sources should be jointly determined to minimize resource consumption. Let $I_{\mathbf{s}}^S(t)$ and $I_{\mathbf{g}}^T(t)$ denote sensing intervals for SSG $\mathbf{s}$ and TSG $\mathbf{g}$ at time slot t, respectively.

B. Age of Information Model for Environment Sensing

As up-to-date sensing results are crucial for CAVs to make timely and accurate decisions in dynamic environments, it is important to satisfy the freshness and reliability requirements of environment sensing. AoI, which is a metric quantifying the time elapsed since the most recent sensing data was generated, can be utilized to describe the freshness and reliability of the sensing results received by CAVs [19]. Specifically, each sensing data is stamped with the time of the generation. The AoI of the sensing result for CAV u is defined as the time elapsed since the latest received sensing result was generated from the LEO satellite or RSU. The evolution of AoI for the sensing result of CAV u can be given by

$$q_u^{\mathbf{x}}(t) = \begin{cases} q_u^{\mathbf{x}}(t-1) + 1, & \text{if no packet received} \\ t - \max_i\{t_u^{\mathbf{x}}(i) | t'^{\mathbf{x}}_u(i) \leq t\}, & \text{otherwise} \end{cases} \quad (1)$$

where $t_u^{\mathbf{x}}(i)$ and $t'^{\mathbf{x}}_u(i)$ are the generation time and the delivered time of the ith sensing data and result of CAV u, and $\mathbf{x} \in \{S, T\}$ represents that the sensing data is generated from satellite or RSUs. When CAV u receives new sensing results, the AoI is renewed to describe the freshness information of the latest data; otherwise, it increases linearly over time slots.

The AoI should be bounded to guarantee the freshness of the environment information. Moreover, to guarantee the reliability of environment sensing, the probability that the sensing data is correctly received within the freshness threshold T^{th} should be larger than $1 - \varepsilon$ [20]. Since CAVs are able to receive sensing results from both RSUs and the LEO satellite, the overall AoI of a CAV depicts the AoI of the data from either source, which is determined by the minimum AoI from terrestrial or satellite networks, as shown in Fig. 2. Note that if a fresher sensing result is received by the CAV, the earlier generated data from either RSUs or LEO satellite for this CAV, which has not been received, will be discarded. In addition, if two sensing results are received at the same time, the formerly generated packet will be discarded. The overall AoI for CAV u can be given as

$$q_u(t) = \min\{q_u^S(t), q_u^T(t)\}. \tag{2}$$

From Fig. 2, we can find that both sensing interval and delay of data processing and transmission can affect the AoI value. Therefore, we need to jointly optimize the sensing interval for SGs and the allocation of computing and communication resources from both satellite and terrestrial networks to satisfy the freshness requirements of environment sensing.

C. Computing and Communication Model

When the sensing data is generated for each SG, it needs to be processed and then the result needs to be transmitted to CAVs. For each SSG, the initial sensing data size to be processed is denoted by $\nu_{\mathbf{s}}^S(t)$, which varies for different sensing areas. Let $K(t)+\Psi_{\mathbf{s}}^S(t)+iI_{\mathbf{s}}^S(t)$ represent the generation time of the ith sensing data, where $K(t) = \max\{jk \,|\, jk \leq t \;\; \forall j\}$ is the initial time slot of the current interval for adjusting SSGs, and $\Psi_{\mathbf{s}}^S(t)$ is a delayed time of the first sensing for SSG $\mathbf{s}$ from $K(t)$. The satellite computing resources allocated for SSG $\mathbf{s}$ at time slot t is denoted by $c_{\mathbf{s}}^S(t)$. Let $Q_{\mathbf{s}}^S(t)$ indicate the size of remaining data for processing at time slot t for SSG $\mathbf{s}$, as given in (3), shown at the bottom of the page. The amount of data processed at time slot t for SSG $\mathbf{s}$ is determined by $\Delta\nu_{\mathbf{s}}(t) = \min\{Q_{\mathbf{s}}^S(t), \tau f^S c_{\mathbf{s}}(t)/\gamma\}$, where f^S represents the CPU frequency unit (in CPU cycles per second) and γ is the computation workload (in CPU cycles per bit). Specifically, the following computing resource allocation constraints should be satisfied:

$$\sum_{\mathbf{s}\in\Omega^S(t)} c_{\mathbf{s}}^S(t) \leq c_{\max}^S \quad \forall t \tag{4}$$

$$c_{\mathbf{s}}^S(t) = c_{\mathbf{s}}^S(t-1), \quad \text{if } 0 < Q_{\mathbf{s}}^S(t) < Q_{\mathbf{s}}^S(t-1) \tag{5}$$

where (4) indicates the constraint on the maximum computing resources in the LEO satellite, and (5) represents that the allocated computing resources remain unchanged during the processing.

After processing the sensing data, the sensing results need to be multicast to CAVs in each SSG, where the data size of the sensing results for SSG $\mathbf{s}$ is denoted by $\beta_s^S(t)$. Let $W_{\mathbf{s}}^S(t)$ denote the size of remaining transmission data for SSG $\mathbf{s}$ at time slot t, as expressed in (6), shown at the bottom of the page. In time slot t, the amount of transmitted data is $\Delta\beta_{\mathbf{s}}(t) = \min\{W_s^S(t), \tau R_{\mathbf{s}}^S(t)\}$, where $R_{\mathbf{s}}^S(t) = b_{\mathbf{s}}^S(t)\log_2(1 + [P^S h_{\mathbf{s}}^S(t)]/\sigma^2)$ is the data transmission rate. Here, $b_{\mathbf{s}}^S(t)$ is the bandwidth resources allocated to SSG $\mathbf{s}$ at time slot t, P^S denotes the transmit power of the LEO satellite, σ^2 is the noise power, and $h_{\mathbf{s}}^S(t)$ is the channel gain. The communication resource allocation should satisfy

$$\sum_{\mathbf{s}\in\Omega^S(t)} b_{\mathbf{s}}^S(t) \leq b_{\max}^S \quad \forall t \tag{7}$$

$$b_{\mathbf{s}}^S(t) = b_{\mathbf{s}}^S(t-1), \quad \text{if } 0 < W_{\mathbf{s}}^S(t) < W_{\mathbf{s}}^S(t-1) \tag{8}$$

where (7) constrains the available communication resources of the LEO satellite and (8) represents that the allocated communication resources remain unchanged during the transmission.

Considering the high LEO satellite altitude, the propagation delay cannot be neglected. At time slot t, the remaining propagation time is given by

$$Z_{\mathbf{s}}^S(t) = \begin{cases} T_{\mathbf{s}}^{\text{prop}}(t), & \text{if } W_{\mathbf{s}}^S(t-1) > W_{\mathbf{s}}^S(t) = 0 \\ \max\{Z_{\mathbf{s}}^S(t-1) - \tau, 0\}, & \text{otherwise} \end{cases} \tag{9}$$

where $T_{\mathbf{s}}^{\text{prop}}(t) = \sqrt{|\mathbf{p}^S(t) - \mathbf{p}_{\mathbf{s}}^{\text{SSG}}(t)|^2}/c$ is the propagation delay between SSG $\mathbf{s}$ and the satellite, with the coordination for the center of SSG $\mathbf{s}$ denoted by $\mathbf{p}_{\mathbf{s}}^{\text{SSG}}(t)$ and the light speed being c.

For the TSG served by each RSU, the processing and transmission models are similar. However, the allocated computing and communication resources c^T and b^T to serve TSG $\mathbf{g}$ are fixed to process and transmit data, since the RSU resources are not shared by other TSGs, and no propagation delay is considered.

IV. Problem Formulation and Decomposition

In this section, we formulate the resource scheduling problem to support environment sensing for CAVs, aiming to minimize the resource cost while satisfying freshness and reliability requirements in the presence of network dynamics.

Let $\Omega^S = \{\Omega^S(t) \;\; \forall t \in \mathcal{T}\}$ denote SSGs, and $\mathcal{I}^S = \{I_{\mathbf{s}}^T(t) \;\; \forall \mathbf{s} \in \Omega^S(t) \;\; \forall t\}$ and $\mathcal{I}^T = \{I_{\mathbf{g}}^T(t) \;\; \forall \mathbf{g} \in \Omega^T(t) \;\; \forall t\}$ denote sensing intervals of all SSGs and TSGs in T time slots, respectively. The resource cost for SSG $\mathbf{s}$ at time slot t from the LEO satellite is given by $\Upsilon_{\mathbf{s}}^S(t) = \chi_1^S c_{\mathbf{s}}^S(t) + \chi_2^S b_{\mathbf{s}}^S(t)$, where χ_1^S, χ_2^S are the unit cost of computing and communication resources from the satellite. Similarly, for TSG $\mathbf{g}$ in terrestrial networks, the resource consumption at time slot t is given by $\Upsilon_{\mathbf{g}}^T(t) = \chi_1^T c_{\mathbf{g}}^T(t) + \chi_2^T b_{\mathbf{g}}^T(t)$, where χ_1^T and χ_2^T are the unit cost of computing and communication resources from the RSU. Let $\mathcal{C}^S = \{c_{\mathbf{s}}^S(t) \;\; \forall \mathbf{s} \in \Omega^S \;\; \forall t\}$ and $\mathcal{B}^S = \{b_{\mathbf{s}}^S(t) \;\; \forall \mathbf{s} \in \Omega^S \;\; \forall t\}$ denote the computing and communication resource

$$Q_{\mathbf{s}}^S(t) = \begin{cases} \nu_{\mathbf{s}}^S(t), & \text{if} t = K(t) + iI_{\mathbf{s}}^S(t) + \Psi_{\mathbf{s}}^S(t) \;\; \forall i \\ \max\{Q_{\mathbf{s}}^S(t-1) - \Delta\nu_{\mathbf{s}}(t-1), 0\}, & \text{otherwise} \end{cases} \tag{3}$$

$$W_{\mathbf{s}}^S(t) = \begin{cases} \beta_{\mathbf{s}}^S(t), & \text{if} Q_{\mathbf{s}}^S(t-1) > Q_{\mathbf{s}}^S(t) = 0, \\ \max\{W_{\mathbf{s}}^S(t-1) - \Delta\beta_{\mathbf{s}}(t-1), 0\}, & \text{otherwise} \end{cases} \tag{6}$$

allocation decisions for all time slots, respectively. Note that the unit costs of computing and communication resources vary across the heterogeneous satellite and terrestrial networks, necessitating a cooperative optimization of both terrestrial and satellite resource costs for environment sensing in STVN. In this case, the goal is to minimize overall resource costs while guaranteeing the freshness and reliability of sensing data for CAVs, which can be formulated as

$$\mathbf{P1} \min_{\substack{\Omega^S, \mathcal{C}^S, \\ \mathcal{B}^S, \mathcal{I}^S, \mathcal{I}^T}} \sum_{t=1}^{T} \left(\sum_{\mathbf{s} \in \Omega^S} \Upsilon_{\mathbf{s}}^S(t) + \sum_{\mathbf{g} \in \Omega^T} \Upsilon_{\mathbf{g}}^T(t) \right) \tag{10}$$

$$\text{s.t.} \quad \frac{\sum_{t'=1}^{t} \mathbb{1}_{q_u(t') \geq T^{\text{th}}}}{t} < \varepsilon \ \forall u \in \mathcal{U} \quad \forall t \in \mathcal{T} \tag{10a}$$

$$\mathbf{s}_i \cap \mathbf{s}_j = \emptyset \quad \forall \mathbf{s}_i, \mathbf{s}_j \in \Omega^S(t), i \neq j \tag{10b}$$

$$\cup_{\mathbf{s} \in \Omega^S(t)} \mathbf{s} = \mathcal{U} \tag{10c}$$

$$I_{\mathbf{s}}^T(t), I_{\mathbf{g}}^T(t) \in \{l\kappa | l \in \mathbb{N}\} \tag{10d}$$

$$|\Omega^S(t)| \leq M$$

$$(4), (5), (7), (8). \tag{10e}$$

In **P1**, (10a) represents the freshness and reliability requirement that the probability of task failure should be less than the threshold ε over any accumulated period of t time slots; (10b) and (10c) constrain the SSGs served by the LEO satellite, where CAVs cannot be simultaneously served in multiple SSGs and every CAV in the target area should be included in one SSG; and (10d) constrains the available sensing interval for each SG, where κ is the minimum sensing interval limited by sensing devices. Considering the limited capacity of the LEO satellite with the edge server threads of M, indicating the maximum concurrent processing of sensing data [21], (10e) regulates the maximum number of SSGs.

Solving **P1** encounters the following challenges. Determining the resource allocation in each time slot is a sequential decision problem, where the decision at a time slot will affect the subsequent decisions. Moreover, determining long-term SSGs and sensing interval decisions, along with the short-term resource allocation decisions, is a mixed-integer optimization problem, where two types of variables are mutually dependent. In this case, directly applying model-free techniques can exacerbate model convergence difficulties, especially considering the highly dynamic network environment and the high-dimensional action space. To address these challenges, we propose a CSTRS scheme, which employs a data-model co-driven approach to solve the problem.

Considering the characteristics of the action, adjusting SSGs and the sensing interval is a long-term action for each time interval, and the resource allocation decisions are short-term actions determined in each time slot. Therefore, we decouple the original problem into two subproblems: 1) CAV partitioning and sensing interval decisions determined by the ground controller and 2) real-time computing and communication resource allocation for SGs in the satellite and RSUs. Fig. 3 shows the working diagram of the proposed CSTRS scheme for environment sensing in STVN in two steps.

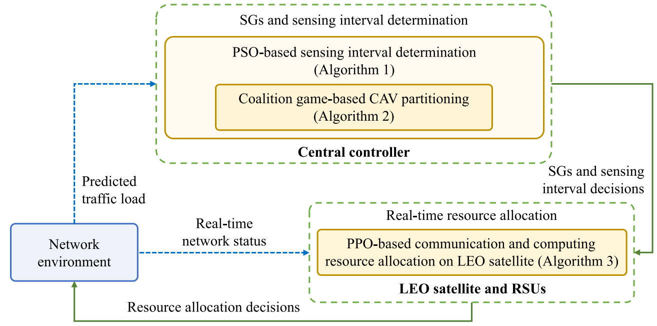

Fig. 3. Working diagram of the proposed CSTRS scheme for environment sensing.

In the first subproblem, we aim to find the optimal CAV partitioning and sensing intervals for each SG to minimize resource consumption in each time interval consisting of k time slots. Specifically, considering the long-term performance in each time interval, the average resource cost of each SG can be estimated through predicted processing and transmission workload according to the predicted CAV trajectories.[1] Therefore, the first subproblem can be given by

$$\mathbf{P2} \min_{\Omega^S, \mathbf{I}^S, \mathbf{I}^T} \sum_{\mathbf{s} \in \Omega^S} C_{\mathbf{s}}^S + \sum_{\mathbf{g} \in \Omega^T} C_{\mathbf{g}}^T$$
$$\text{s.t.} \quad (10b)-(10e). \tag{11}$$

Specifically, $C_{\mathbf{s}}^S$ is the average resource cost for SSG $\mathbf{s}$ in a time interval, calculated by the average communication and computing resource usage with their unit cost, given by

$$C_{\mathbf{s}}^S = \chi_1^S \frac{k\tau \bar{v}_{\mathbf{s}}^S \gamma}{I_{\mathbf{s}}^S f^S} + \chi_2^S \frac{k\tau \bar{\beta}_{\mathbf{s}}^S}{I_{\mathbf{s}}^S \bar{R}_{\mathbf{s}}^S} \tag{12}$$

where $I_{\mathbf{s}}^S$ is the sensing interval for SSG $\mathbf{s}$ and $\bar{R}_{\mathbf{s}}^S$ is the average transmission rate of unit spectrum bandwidth within the time interval. Here, $\bar{v}_{\mathbf{s}}^S$ and $\bar{\beta}_{\mathbf{s}}^S$ denote the predicted processing and transmission workloads for each sensing of SSG $\mathbf{s}$ in the time interval, respectively. Similarly, the average resource cost for TSG $\mathbf{g}$ in a time interval can be represented by

$$C_{\mathbf{g}}^T = \chi_1^T \frac{k\tau \bar{v}_{\mathbf{g}}^T \gamma}{I_{\mathbf{g}}^T f^T} + \chi_2^T \frac{k\tau \bar{\beta}_{\mathbf{g}}^T}{I_{\mathbf{g}}^T \bar{R}_{\mathbf{g}}^T}. \tag{13}$$

Then, given the CAV partitioning and sensing intervals, in the second subproblem, we aim to find the optimal sequential decision of resource allocation to minimize the overall resource cost based on the real-time network state, given as

$$\mathbf{P3} \min_{\mathcal{C}^S, \mathcal{B}^S} \sum_{t=1}^{T} \left(\sum_{\mathbf{s} \in \Omega^S(t)} \Upsilon_{\mathbf{s}}^S(t) + \sum_{\mathbf{g} \in \Omega^T(t)} \Upsilon_{\mathbf{g}}^T(t) \right)$$
$$\text{s.t.} \quad (4), (5), (7), (8), (10a). \tag{14}$$

To solve these two subproblems, the proposed CSTRS scheme comprises two components: 1) a CAV partitioning and sensing interval determination algorithm presented in Section V, and 2) a real-time resource allocation algorithm, detailed in Section VI.

[1]Note that, the prediction method is not the primary focus of this article and several algorithms have been studied for this purpose, such as recurrent neural networks (RNNs) [22], convolutional neural networks (CNNs), and long-short term memory (LSTM) [23].

V. CAV Partitioning and Sensing Interval Determination

To find the optimal SSGs and the sensing interval of each group, in this section, we design a two-step algorithm to solve subproblem **P2**. Specifically, the feasible sensing interval for each CAV is first derived according to the freshness requirement. Then, to achieve the minimum estimated average resource cost in each time interval, we investigate a PSO-based method to find the optimal sensing intervals for CAVs and determine the SSGs by formulating a coalition formation game in each time interval.

A. PSO-Based Sensing Interval Determination

For each CAV, let $T_u^S(t)$ and $T_u^T(t)$ denote the sensing interval from the LEO satellite and connected RSUs for CAV u at time slot t, respectively. Specifically, $T_u^S(t)$ and $T_u^T(t) \bmod \kappa = 0$ follow the minimum interval limited by the sensing devices. For simplicity, we omit the notation t in this section, as decisions are adjusted in each time interval consisting of k time slots. To guarantee the sensing data freshness requirement for each CAV, some preliminary conditions on the sensing intervals should be satisfied according to the maximum allowable AoI requirement.

Proposition 1 (Feasible Sensing Interval Pair for Individual CAVs): The sensing interval pair for CAV u is denoted by (T_u^S, T_u^T), with an offset of ψ_u^S. Here, the offset is the delayed time of the initial satellite sensing from the initial RSU sensing in a time interval, where the initial RSU sensing time is at the beginning of a time interval. To satisfy the freshness requirement of environment sensing, the sensing interval pair of each CAV must guarantee the following conditions.

1) If CAV u cannot connect to RSUs either partially or completely during the time interval, i.e., $a_u^T(t) = 0, \exists t$, the sensing interval from the satellite should guarantee $T_u^S < T^{\text{th}}$, with $\hat{\psi}_u^S = [0, T_u^S)$.
2) If CAV u can always connect to both the LEO satellite and RSUs during the time interval, the sensing interval pair should meet one of the following conditions.
   a) $T_u^S < T^{\text{th}}$, with $\psi_u^S \in \hat{\psi}_u^S = [0, T_u^S)$.
   b) $T_u^T < T^{\text{th}}$, with $\psi_u^S \in \hat{\psi}_u^S = [0, T_u^T)$.
   c) $T_u^S = T_u^T \in [T^{\text{th}}, 2T^{\text{th}})$, with $\psi_u^S \in \hat{\psi}_u^S = \{l\kappa \mid l\kappa \in (T_u^T - T^{\text{th}}, T^{\text{th}}) \;\; \forall l \in \mathbb{N}\}$.

where $\hat{\psi}_u^S$ is the set of feasible offset for CAV u.

Proof: The proof is given in the Appendix. ■

With the feasible value ranges for individual CAVs' sensing interval pairs and satellite sensing time offset given in Proposition 1, we can then determine the sensing intervals of all SGs to achieve the optimum of problem **P2**. Note that determining the sensing interval for each SG is a combinatorial optimization problem and finding a globally optimal solution is challenging [24]. To address this issue, we employ PSO, an evolutionary heuristic mechanism, to solve problem **P2**. In this approach, a set of particles form a particle swarm. Each particle's position represents a solution for CAVs' sensing interval pairs, denoted by $\Lambda = [T_u^S, T_u^T]^{1\times|\mathcal{U}|}$. In each iteration, particles adjust their positions and speeds within the solution space to discover the corresponding values from the current positions [24]. After multiple iterations, the positions of all particles can converge to the same position indicating the selected sensing interval pair for all CAVs [25].

Algorithm 1 PSO-Based Sensing Interval Determination

Input: Ω^T, σ, σ_1, σ_2, $y^{\max}$;
Initialization: $y = 0$, $p_x^{(0)} = 0$, $\Lambda_x^{(0)} \in \mathbb{F}, \forall x \in \mathcal{X}$;
while $y \le y^{\max}$ **do**
  for $x \in \mathcal{X}$ **do**
    if Proposition 1 and Eq. (17) are not satisfied **then**
      Replace the particle by a new $\Lambda_x^{(y)} \in \mathbb{F}$;
    Obtain sensing intervals $\mathbf{I}_x^{T,(y)}$ of TSGs according to Eq. (17);
    Determine $\Omega_x^{S,(y)}$ and $\mathbf{I}_x^{S,(y)}$ based on Algorithm 2 and calculate $\Xi_x^{(y)}$;
    if $\Xi_x^{(y)} < \hat{\Xi}_x$ **then**
      Update $\hat{\Lambda}_x \leftarrow \Lambda_x^{(y)}$, $\hat{\Xi}_x \leftarrow \Xi_x^{(y)}$;
    if $\Xi_x^{(y)} < \Xi^*$ **then**
      Update $\Lambda^* \leftarrow \Lambda_x^{(y)}$, $\Xi^* \leftarrow \Xi_x^{(y)}$;
    Update $p_x^{(y+1)}$ based on (15);
    Select $\Lambda_x^{(y+1)}$ based on (16);
Output: Ω^S, $\mathbf{I}^S$, and $\mathbf{I}^T$

Denote the set of particles and the position of particle x in yth iteration by $\mathcal{X}$ and $\Lambda_x^{(y)}$, respectively. Let $\hat{\Lambda}_x$ and Λ^* denote the best position of particle x and the best position among all particles' positions up to the latest iteration, respectively, and $\hat{\Xi}_x$ and Ξ^* are the corresponding values calculated based on (11) at those positions. The speed of particle $x \in \mathcal{X}$ in the yth iteration, denoted by $p_x^{(y)}$, is updated as

$$p_x^{(y)} = \sigma p_x^{(y-1)} + \sigma_1\left(\hat{\Lambda}_x - \Lambda_x^{(y-1)}\right) + \sigma_2\left(\Lambda^* - \Lambda_x^{(y-1)}\right) \quad (15)$$

where σ is the inertia weight for each particle to keep its speed from the previous iteration. σ_1 and σ_2 are the cognitive coefficient and the social coefficient to control how much weight should be given to refining the search result of the particle itself and recognizing the search result of the swarm consisting of the randomness for exploration [25]. The position of particle x in yth iteration is given by

$$\Lambda_x^{(y)} = \Lambda_x^{(y-1)} + p_x^{(y-1)}. \quad (16)$$

For the PSO-based algorithm, each particle should explore the solution within the solution space $\Lambda \in \mathbb{F}$. Specifically, since TSGs are predefined according to the coverage of RSUs, CAVs in the same TSG should have the same sensing interval, given by

$$T_{u_1}^T = T_{u_2}^T = I_{\mathbf{g}}^T \quad \forall u_1, u_2 \in \mathbf{g}. \quad (17)$$

Moreover, all sensing interval pairs in a possible solution of particle positions should fulfill Proposition 1. If a particle moves out of the solution space $\mathbb{F}$, it will be replaced by a new particle. In other words, all sensing interval pairs violating Proposition 1 and (17) are replaced by new randomly selected sensing interval pairs, for the exploration in the solution space.

The details of the proposed PSO-based algorithm are given in Algorithm 1. Denote the maximum number of iterations by $y^{\max}$. The particles are initialized with the positions in the solution space $\mathbb{F}$ in line 2. The position of each particle is updated in each iteration according to lines 5–14. Specifically, with a given position, i.e., the sensing interval pair of each CAV, SSGs Ω^S and the corresponding sensing interval $\mathbf{I}^S$ can be obtained through the coalition game-based partitioning algorithm, which will be presented in Section V-B. Finally, the outputs of the PSO-based algorithm are the solution of **P2** for each time interval.

B. Coalition Game-Based CAV Partitioning Algorithm

Considering the coverage of RSUs, TSGs are predefined at the beginning of each time interval and the RSU sensing interval can be determined based on (17). On the other hand, the optimal SSGs and the corresponding sensing interval still remain to be determined to solve **P2** with minimum resource costs. Recall that the satellite sensing interval for each CAV within an SSG can be calculated according to Algorithm 1 and may vary among different CAVs. The sensing interval of SSG and the corresponding available offset can be given as follows.

Proposition 2 (Sensing Interval and Offset Values of an SSG): Given the sensing interval and feasible offset values of each CAV within an SSG, the sensing interval of SSG $\mathbf{s}$ $I^S_{\mathbf{s}}$ and the offset $\Psi^S_{\mathbf{s}}$ can be obtained according to the following two cases.

1) If all CAVs in SSG $\mathbf{s}$ have the same sensing interval and common offset values, given by

$$\begin{cases} T^S_{u_1} = T^S_{u_2} \ \forall u_1, u_2 \in \mathbf{s} \\ \bigcap_{u\in\mathbf{s}} \hat{\psi}^S_u \neq \emptyset \end{cases} \tag{18}$$

then the sensing interval of SSG $\mathbf{s}$ is $I^S_{\mathbf{s}} = T^S_u \ \ \forall u \in \mathbf{s}$, and the offset of the SSG is $\Psi^S_{\mathbf{s}} = \arg\max_{\varphi\in\hat{\Psi}^S_{\mathbf{s}}} |T^{\text{th}} - \varphi|$ to maximize the allowable delay for data processing and transmission of each satellite sensing. Here, $\hat{\Psi}^S_{\mathbf{s}} = \bigcap_{u\in\mathbf{s}} \hat{\psi}^S_u$ is the common feasible SSG sensing offset set.

2) Otherwise, the sensing interval of SSG $\mathbf{s}$ is $I^S_{\mathbf{s}} = \max\{l\kappa \mid l\kappa < T^{\text{th}}, l \in \mathbb{N}^+\}$ with the offset $\Psi^S_{\mathbf{s}} = 0$.

Note that employing a centralized approach to find the optimal SSGs through a complete search for all possible solutions encounters high complexity. Thus, the coalition game theory emerges as a suitable method to find the optimal partition of CAVs served by the LEO satellite [26].

Definition 1 (The Coalition Partition): A coalition partition is defined as the set $\Gamma^S = \{\mathbf{s}_0, \mathbf{s}_1, \ldots, \mathbf{s}_m\}$, which partitions the CAV set $\mathcal{U}$ into m coalitions, where $0 \leq m \leq M$. Each coalition, defined as an SSG, is disjoint such that $\forall \mathbf{s}_i, \mathbf{s}_j \in \Gamma^S, i \neq j, \mathbf{s}_i \cap \mathbf{s}_j = \emptyset$ and $\bigcup_i \mathbf{s}_i = \mathcal{U}$.

The CAV partition problem can be modeled as a $(\mathcal{U}, \phi)$ coalition game. Here, $\phi(\mathbf{s})$ is the utility function of SSG $\mathbf{s}$, which is the negative value of the estimated resource cost from the LEO satellite in the time interval, given by

$$\phi(\mathbf{s}) = -C^S_{\mathbf{s}}. \tag{19}$$

To minimize the estimated resource cost from the LEO satellite for all SSGs, we aim to find the optimal partition $\tilde{\Gamma}^S$ to maximize the total utility so that

$$\phi\left(\tilde{\Gamma}^S\right) > \phi\left(\Gamma^S\right) \ \ \forall \Gamma^S \neq \tilde{\Gamma}^S \tag{20}$$

where $\phi(\Gamma^S) = \sum_{\mathbf{s}\in\Gamma^S} \phi(\mathbf{s})$ is defined as the total utility of coalitions. One key approach in coalition formation is enabling CAVs to join or leave a coalition based on their preferences, aiming to achieve the highest utility. To assess the preference, the concept of preference relation is introduced below.

Definition 2 (Preference Relation): For any CAV u, a preference relation is defined by $\succ_u$, where $\mathbf{s}_i \succ_u \mathbf{s}_j$ implies that CAV u strictly prefers to join coalition $\mathbf{s}_i$ over $\mathbf{s}_j$.

Specifically, the preference relation for CAV u is given as

$$\mathbf{s}_i \succ_u \mathbf{s}_j \Leftrightarrow \phi(\mathbf{s}_i) + \phi\big(\mathbf{s}_j \backslash \{u\}\big) > \phi\big(\mathbf{s}_j\big) + \phi(\mathbf{s}_i \backslash \{u\}) \tag{21}$$

where $\mathbf{s}_i$ and $\mathbf{s}_j$ are the two potential coalitions containing CAV u. When CAV u finds a more preferable coalition, it can join the new coalition through the switch operation as defined below.

Definition 3 (Switch Operation): Considering a CAV partition Γ^S, if CAV u in coalition $\mathbf{s}_1$ can switch to coalition $\mathbf{s}_2$ to achieve a higher utility based on the preference relation, i.e., $\mathbf{s}_2 \cup \{u\} \succ_u \mathbf{s}_1$, a switch operation occurs. Correspondingly, the partition is modified as follows:

$$\Gamma^S = \left(\Gamma^S \backslash \{\mathbf{s}_1, \mathbf{s}_2\}\right) \cup \{\mathbf{s}_1 \backslash \{u\}\} \cup \{\mathbf{s}_2 \cup \{u\}\}. \tag{22}$$

With a sequence of switch operations, CAVs can detach from their current coalitions and join new coalitions until a stable partition is achieved, defined as follows.

Definition 4 (Stability): A partition is Nash-stable if no CAV tends to change the belonging of the coalition in the current partition [27].

Based on these definitions, we design a coalition formation game-based algorithm for CAV partitioning, with the main workflow given in Algorithm 2. At the initial step, CAVs are partitioned into M coalitions, which is the maximum number of coalitions that can be supported by the satellite. Then, as shown in lines 4–9, it is determined whether a CAV should switch the coalition for a higher utility. $\mathcal{H}(u)$ indicates the history set of coalitions where CAV u has previously joined to avoid repetition. Based on Definition 3, each CAV can detach from the current coalition and join a new coalition, until a stable partition is obtained as per Definition 4. Finally, SSGs are determined by $\Omega^S = \Gamma^S$ with the sensing interval of all coalitions and their corresponding offset according to Proposition 2.

C. Computational Complexity Analysis

In Algorithm 1, PSO is used to determine the sensing interval for each CAV. In each iteration of the proposed PSO-based algorithm, the positions of each particle are updated with the computational complexity of $O(|\mathcal{X}|NU)$, where $|\mathcal{X}|$ is the number of particles and NU represents the dimension of each particle. Specifically, each particle's position encodes the sensing interval pairs for CAVs, which include the sensing interval

Algorithm 2 Coalition Formation Game-Based Algorithm for CAV Partitioning

1: **Input:** $\mathcal{U}$, Λ;
2: **Initialization:** The initial partition of CAVs is Γ^S_{ini}, where CAVs are partitioned into M coalitions;
3: **repeat**
4: Randomly select CAV u and choose another coalition $\mathbf{s} \in \Gamma^S$;
5: **if** CAV prefers to join a new coalition $\mathbf{s}$ **and** $\mathbf{s} \cup \{u\} \notin \mathcal{H}(u)$ **then**
6: Add $\mathbf{s} \cup \{u\}$ to the history set $\mathcal{H}(u)$;
7: CAV u detaches the current coalition and combines with the new coalition according to Definition 3;
8: Update partition Γ^S;
9: **until** Switch operation terminates with a stable partition
10: **Output:** Final SSGs $\Omega^S = \Gamma^S$, the sensing interval of all coalitions $\{I^S_1, ..., I^S_m\}$, and the offset $\{\Psi^S_1, \ldots, \Psi^S_m\}$ according to Proposition 2.

from both the satellite and RSU. Since CAVs within the same TSG share the same RSU sensing interval given in (17) and there are N RSUs in the target area, the dimensionality of each particle is NU. After determining the sensing interval of each CAV, a coalition game is used to partition CAVs into different SSGs in Algorithm 2. In the coalition game, the maximum number of CAV selections is UM. In the worst case, each CAV is evaluated against $M-1$ coalitions in each iteration. This results in a computational complexity of $O(UM^2)$ for each iteration of the coalition game. Therefore, the overall computational complexity for determining CAV partitions and sensing intervals for each SG is $O(L_1|\mathcal{X}|(NU + L_2UM^2))$, where L_1 and L_2 are the finite number of iterations required for the PSO and coalition game to converge.

VI. PPO-Based Real-Time Resource Allocation Algorithm

With the determined SSGs and sensing intervals, the LEO satellite needs to allocate computing and communication resources for processing sensing data and transmitting sensing results to CAVs in each SSG. In this section, we reformulate **P3** by leveraging the Markov decision process (MDP) and propose a reinforcement learning-based algorithm to solve the problem.

A. Markov Decision Process Formulation

Since (10a) in **P3** is related to long-term delay and reliability requirement, it is challenging to solve the sequential decision problem directly. To decompose the long-term impact of the delay and reliability in each time slot, we construct a virtual reliability queue based on the Lyapunov optimization technique [28]

$$H_u(t+1) = \max\{H_u(t) + \mathbb{1}_{q_u(t)>T^{\text{th}}} - \varepsilon, 0\} \tag{23}$$

where $\mathbb{1}_{\text{condition}} = 1$ if *condition* is true and $\mathbb{1}_{\text{condition}} = 0$ otherwise, and $H_u(1) = 0$. When the AoI for CAV u violates the freshness requirement at time slot t, the virtual reliability queue $H_u(t+1)$ enlarges at time slot $t+1$. On the other hand, the virtual reliability queue will decrease if a new sensing result is received within the freshness requirement. As a historical measurement of freshness-related task failures, the virtual reliability queue reflects the deviation of the current failure rate from the reliability constraint. Therefore, the long-term delay and reliability constraint is transformed into guaranteeing the stability of the virtual reliability queue. Let $H^{\max}_{\mathbf{s}}(t)$ denote the group-based virtual queue value reflecting the reliability of SSG $\mathbf{s}$, which is the maximal virtual reliability queue value of CAVs in the SSG, given by $H^{\max}_{\mathbf{s}}(t) = \max_{u\in\mathbf{s}} H_u(t)$. Therefore, we can transform optimization problem **P3** into

$$\begin{aligned}\mathbf{P4}\ \min_{\mathcal{C}^S,\mathcal{B}^S}\ & \sum_{t=1}^{T}\left(\sum_{\mathbf{s}\in\Omega^S(t)}\left(\Upsilon^S_{\mathbf{s}}(t) + \eta H^{\max}_{\mathbf{s}}(t)\right) + \sum_{\mathbf{g}\in\Omega^T(t)} \Upsilon^T_{\mathbf{g}}(t)\right)\\ \text{s.t.}\ & (4), (5), (7), (8)\end{aligned} \tag{24}$$

where the weight value η is used to balance the resource cost and the reliability.

Since the formulated computing and communication resource allocation problem **P4** is an integer nonlinear optimization problem with random channel conditions and dynamic mobility of CAVs, it cannot be solved by deterministic optimization algorithms. Thus, we reformulate **P4** by leveraging MDP to model the randomness of channels and CAV mobility.

Let $\zeta_{\mathbf{s}}(t) = [\mathbf{p}^{\text{SSG}}_{\mathbf{s}}(t), q^{\max}_{\mathbf{s}}(t), H^{\max}_{\mathbf{s}}(t), Q^S_{\mathbf{s}}(t), W^S_{\mathbf{s}}(t), c^S_{\mathbf{s}}(t-1), b^S_{\mathbf{s}}(t-1)]$ denote the state of SSG $\mathbf{s}$ at time slot t, where $q^{\max}_{\mathbf{s}}(t) = \max_{u\in\mathbf{s}}\{q_u(t)\}$. Considering the varying SSG numbers in different time intervals, the variability in state and action spaces for all SSGs poses a challenge in solving the problem. Therefore, we use the maximum number M to regulate the overall state and action spaces for all SSGs. The overall state at time slot t is denoted by $\mathcal{S}(t) = [\zeta_{\mathbf{s}_1}(t), \ldots, \zeta_{\mathbf{s}_M}(t)] \in \mathfrak{S}$, where $\mathfrak{S}$ is the state space with all possible states. If the SSG number $|\Omega^S(t)| < M$, $\zeta_{\mathbf{s}_i}(t) = [0]_{1\times|\zeta_{\mathbf{s}_i}|}\ \forall i > |\Omega^S(t)|$.

Let $\mathfrak{A} = \mathfrak{A}^c \otimes \mathfrak{A}^b$ denote the action space, formed by combining the action spaces for the computing and communication resource allocation, where $\otimes$ is the Cartesian product. Thus, the action at time slot t is denoted by $\mathcal{A}(t) = \{(c^S_{\mathbf{s}_1}(t), b^S_{\mathbf{s}_1}(t)), \ldots, (c^S_{\mathbf{s}_M}(t), b^S_{\mathbf{s}_M}(t))\} \in \mathfrak{A}$, where the action space is continuous with $\mathcal{A}(t) \in ([0, 1] \times [0, 1])^{1\times M}$.

To evaluate an action with a given state, the set of rewards is denoted by $\mathfrak{R} := \mathfrak{S} \times \mathfrak{A} \to \mathbb{R}$. We define the reward function obtained from taking action $\mathcal{A}(t)$ in state $\mathcal{S}(t)$ as

$$\begin{aligned}\mathcal{R}(\mathcal{S}(t), \mathcal{A}(t)) = & -\sum_{\mathbf{s}\in\Omega^S(t)}\left(\Upsilon^S_{\mathbf{s}}(t) + \eta H^{\max}_{\mathbf{s}}(t)\right)\\ & -\sum_{\mathbf{g}\in\Omega^T(t)} \Upsilon^T_{\mathbf{g}}(t).\end{aligned} \tag{25}$$

Let Π denote the set of all policies, which is the function mapping from state space $\mathfrak{S}$ to action space $\mathfrak{A}$. To estimate the expected return of the current decision making, a discounted cumulative reward function is considered and the objective function is transformed as

$$\max_{\pi \in \Pi} \mathbb{E}\left[\sum_{t=1}^{T} \iota^t \mathcal{R}(\mathcal{S}(t), \mathcal{A}(t)) \middle| \pi \right] \tag{26}$$

where $\iota \in (0, 1)$ is a discounted factor to reflect the importance of future rewards compared with immediate rewards.

B. PPO-Based Algorithm for Resource Allocation

Considering the lack of information on state transition probabilities and the continuous action space, the policy gradient-based reinforcement learning is a potential method to solve the MDP-based problem. This method directly updates the policy to maximize the total reward without requiring state transition probabilities. However, the vanilla policy gradient approach often suffers from high variance in parameter updates, leading to substantial policy fluctuation during learning and potential instability. Therefore, we propose to adopt a PPO-based algorithm [29], which can effectively handle large-scale problems while ensuring a stable and reliable training process with its clipped objective function to prevent large policy variations. Specifically, the PPO-based algorithm aims to find the optimal parameter θ for policy π_θ that maximizes the clipped surrogate objective

$$L^{\text{clip}}(\theta) = \mathbb{E}\left\{\min\left(\xi_\theta A^{\pi_{\theta_{\text{old}}}}, \text{clip}(\xi_\theta, 1-\delta, 1+\delta) A^{\pi_{\theta_{\text{old}}}}\right)\right\}. \tag{27}$$

Specifically

$$\xi_\theta = \frac{\pi_\theta(\mathcal{A}|\mathcal{S})}{\pi_{\theta_{\text{old}}}(\mathcal{A}|\mathcal{S})} \tag{28}$$

is the policy updating ratio based on the current policy and $A^{\pi_{\theta_{\text{old}}}}$ is the estimated advantage from the policy $\pi_{\theta_{\text{old}}}$, which can be expressed as

$$\begin{aligned} &A^{\pi_{\theta_{\text{old}}}}(\mathcal{S}(t), \mathcal{A}(t)) \\ &\quad = \mathcal{R}(\mathcal{S}(t), \mathcal{A}(t)) + \iota V_\vartheta(\mathcal{S}(t+1)) - V_\vartheta(\mathcal{S}(t)) \end{aligned} \tag{29}$$

where $V_\vartheta(\mathcal{S}(t))$ is a state-value function parameterized by ϑ, given by

$$V_\vartheta(\mathcal{S}(t)) = \mathbb{E}\left\{\sum_{i=0}^{\infty} \iota^i \mathcal{R}(\mathcal{S}(t+i+1), \mathcal{A}(t+i+1)) | \mathcal{S}(t)\right\}. \tag{30}$$

The clipping function clips the ratio ξ_θ between $1-\delta$ and $1+\delta$ with a clipping hyperparameter δ, which removes incentives for the new policy to get far from the old policy to improve the learning stability.

The overall PPO-based resource allocation algorithm is given in Algorithm 3, where J is the maximum number of episodes and E is the epoch for training. Note that given the diverse scales of components in the state, we perform normalization on each component to improve the stability of the training. First, the policy and the value functions are initialized with parameters θ and ϑ, respectively. The buffer $\mathcal{B}$ is used to store transitions resulting from interactions with the environment. Then, at each time slot, the LEO satellite collects the state from the environment, takes actions based on the current policy, computes the reward, observes the new state, and records transitions into buffer based on lines 5–7. After T time slots, the policy and value function will be updated based on the clipped surrogate objective and the mean-square error based on lines 11–13.

Algorithm 3 PPO-Based Resource Allocation Algorithm

1: **Initialization:** Parameters θ and ϑ for policy and state-value function, and buffer $\mathcal{B}$;
2: **for** $j \in \{1, 2, \ldots, J\}$ **do**
3:   Obtain initial state $\mathcal{S}(1)$;
4:   **for** $t \in \{1, 2, \ldots, T\}$ **do**
5:     Execute action $\mathcal{A}(t)$ based on the policy π_θ;
6:     Compute reward $\mathcal{R}(\mathcal{S}(t), \mathcal{A}(t))$ and observe new state $\mathcal{S}(t+1)$;
7:     Record transition $(\mathcal{S}(t), \mathcal{A}(t), \mathcal{R}(t), \mathcal{S}(t+1))$ into buffer $\mathcal{B}$;
8:     **if** $t \mod k = 0$ **then**
9:       Run Algorithm 1 to adjust sensing interval and CAV partition;
10:   **for** $e \in \{1, 2, \ldots, E\}$ **do**
11:     Sample a minibatch of N transitions from buffer $\mathcal{B}$;
12:     Update the policy parameter $\theta \leftarrow \arg\max_{\theta'} L^{\text{clip}}(\theta')$;
13:     Update state-value function parameter $\vartheta \leftarrow \arg\min_{\vartheta'}(\mathcal{R}(t) + V_\vartheta(\mathcal{S}(t+1)) - V_\vartheta(\mathcal{S}(t)))^2$
14:   Empty buffer $\mathcal{B}$;
15: **Output:** Parameter θ;

VII. Performance Evaluation

In this section, extensive simulations are carried out to evaluate the proposed CSTRS scheme. Specifically, we first elaborate on the simulation settings. Afterward, simulation results are presented to demonstrate the effectiveness of our proposed scheme.

A. Simulation Setting

In our simulation scenario, the target area is a beam coverage of a steerable LEO satellite. The orbit altitude of the LEO satellite is 550 km, and the satellite velocity is 7.56 km/s. CAVs and RSUs are randomly distributed in the area, with the radius of the coverage area of each RSU being 500 m. Specifically, the target area consists of both urban and rural areas, where different areas have different densities of RSUs and CAVs. By default, urban areas have RSU densities of 10 per km^2 and CAV densities of 40 per km^2, while rural areas have RSU densities of 2 per km^2 and CAV densities of 20 per km^2, respectively. In the simulated scenario, CAVs move with stochastic direction and speed in each time slot. The maximum freshness requirement of CAVs is set as 100 ms. The time duration for each time slot is set to be $\tau = 5$ ms and the time interval for adjusting SSGs is 10 s. The minimum sensing interval κ is 20 ms. The default reliability requirement in this simulation is 0.99. More simulation parameters, which are related to the computing and communication of satellites and RSUs [30], [31], [32], are listed in Table III.

TABLE III
SIMULATION PARAMETERS

LEO satellite transmission power P^{S}	40 dBm
LEO satellite antenna gains	32 dBi
LEO satellite bandwidth	250 MHz
LEO satellite path-loss exponent	2.5
CPU frequency in LEO satellite	1 Gcycles/s
RSU transmission power	32 dBm
RSU antenna gains	10 dBi
RSU bandwidth	100 MHz
RSU path-loss exponent	3
CPU frequency in RSU	1 Gcycles/s
Noise power σ^2	-174 dBm/Hz
CAV antenna gains	10 dBi
Unit cost of resources $\chi_1^{\mathrm{S}}, \chi_2^{\mathrm{S}}, \chi_1^{\mathrm{T}}, \chi_2^{\mathrm{T}}$	0.5, 2.5, 0.1, 0.5
Workload of sensing data processing	25 cycles/bit

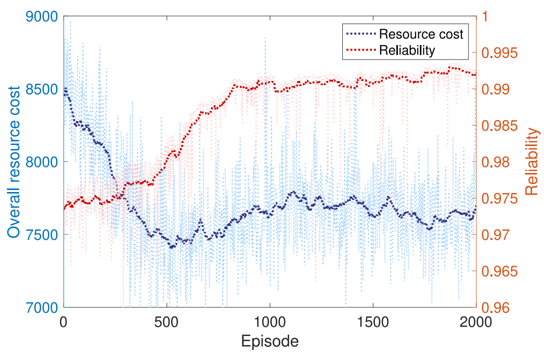

Fig. 4. Convergence performance of the training process.

For the training of the PPO-based reinforcement learning model, the deep neural network utilized in our proposed algorithm includes three fully connected hidden layers with (128, 128, 64) neurons. The ReLU activation function is applied after each hidden layer to realize a nonlinear approximation. Each training episode spans 8000 time slots with CAVs and RSUs randomly reset at the beginning of each episode.

B. Performance of Resource Scheduling for Environment Sensing in STVN

We first present the convergence performance of the proposed CSTRS scheme in terms of resource cost and reliability in each episode of the training period. The simulation comprises 1800 episodes with a learning rate of 3×10^{-4} and a clipping ratio of 0.3. Fig. 4 shows the overall accumulative resource cost and reliability in each episode, which converges after around 1100 episodes.

Next, we perform several experiments to validate the efficacy of each component in CSTRS. We first evaluate the effectiveness of the PPO-based resource allocation algorithm. Specifically, we adopt the following three benchmark algorithms for resource allocation, namely 1) *FCFS*-based allocation [33]: the LEO satellite adopts the first-come-first-serve policy and allocates all available resources to the first requesting SSG; 2) *Random* allocation: the LEO satellite allocates computing and communication resources randomly, only considering the resource capacity constraints; and 3) *Average* allocation [33]: computing and communications resources are allocated equally to each SSG. For *FCFS*-based resource allocation algorithm, if multiple SSGs start to process or transmit sensing data at the same time, all available resources will be allocated equally to serve SSGs.

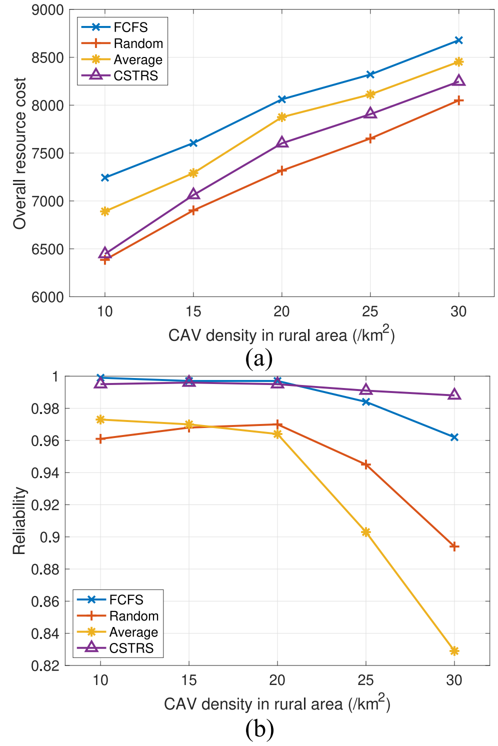

Fig. 5. Performance of different resource allocation algorithms. (a) Resource cost performance. (b) Reliability performance.

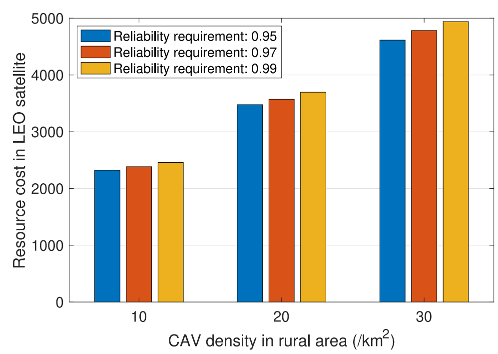

Fig. 6. Resource cost in LEO satellite with different reliability requirements.

Considering that the LEO satellite is essential to providing environment sensing services for CAVs in rural areas, the performances of different resource allocation algorithms under different CAV densities in rural areas are shown in Fig. 5. We can find that our proposed CSTRS scheme can well satisfy the reliability requirements with low resource cost by efficiently allocating resources to adapt to dynamic network environments. When CAV density is small, the *FCFS* algorithm and the CSTRS scheme can both satisfy the reliability requirement of 0.99, whereas our proposed scheme has lower resource cost. With a large CAV density, *FCFS* can hardly guarantee reliability due to the improper resource scheduling policy for different SSGs, while the CSTRS scheme consistently satisfies the reliability requirements.

In Fig. 6, we compare the resource cost in the LEO satellite with different reliability requirements. The results show the

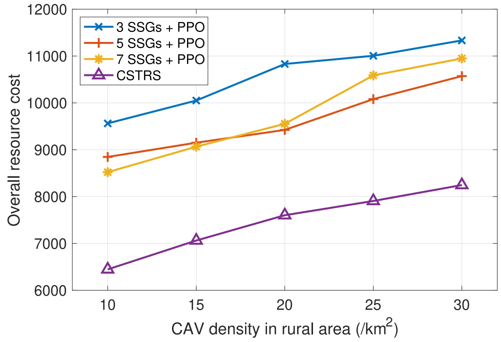

(a)

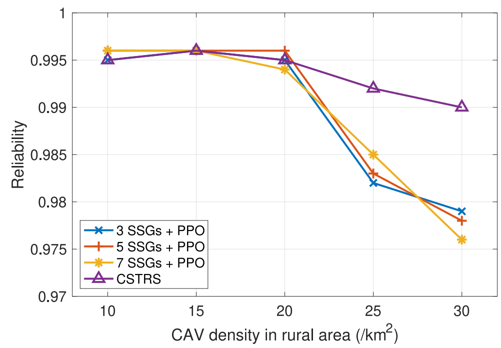

(b)

Fig. 7. Performance of different CAV partition policies. (a) Resource cost performance. (b) Reliability performance.

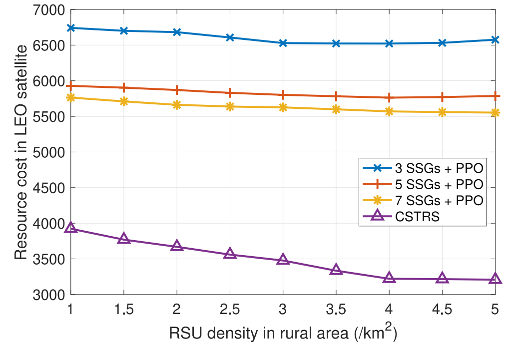

Fig. 8. Resource cost in LEO satellite under different RSU densities in rural area.

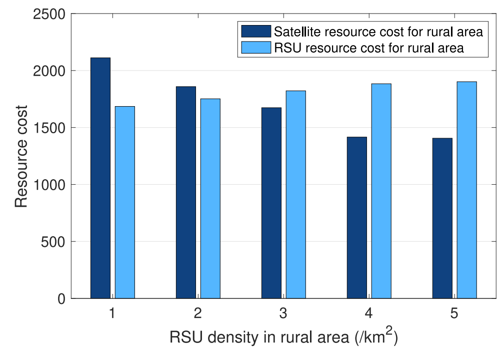

Fig. 9. Resource cost in rural areas from terrestrial and LEO satellite networks.

adaptivity of our proposed CSTRS scheme, which can achieve efficient resource costs with any given reliability requirements by allocating resources for different SSGs.

Next, we investigate the effectiveness of the PSO-assisted sensing interval and CAV partition algorithm in our proposed CSTRS scheme. For comparison, we introduce a benchmark algorithm named *fixed-number SSG*, where the SSG number in the serving area is predetermined and fixed during the simulation. The sensing interval of each SG is determined through Algorithm 1, while SSGs are determined by k-means algorithm based solely on CAV positions at the beginning of each time interval. The communication and computing resources are allocated by adopting the PPO-based algorithm.

In Fig. 7, we compare the resource cost and reliability performances of different CAV partition methods with different CAV densities in rural areas. Specifically, our proposed CSTRS scheme has a low resource cost compared with *fixed-number SSG* strategies. This advantage stems from the adaptive adjustment of CAV partitions and sensing intervals of SGs in the CSTRS scheme based on dynamic environments by jointly considering both LEO satellite and terrestrial networks, enhancing the overall efficiency. With the increment of CAV densities, resource cost increases accordingly, and the CSTRS scheme consistently maintains a low level of resource cost while satisfying reliability requirements. On the other hand, *fixed-number SSG* strategies face challenges in effectively utilizing terrestrial and satellite resources due to improper CAV partitioning and sensing intervals. Particularly, the reliability of *fixed-number SSG* strategies cannot be guaranteed for environment sensing with a high CAV density due to insufficient resources.

In Fig. 8, we compare the LEO satellite resource cost of different CAV partition strategies with different RSU densities in the rural area. From the figure, we observe that the CSTRS scheme consumes less resources in the LEO satellite compared to *fixed-number SSG* policies, due to the joint decision of CAV partition and sensing interval between satellite and terrestrial networks. Moreover, when RSU density increases, the LEO satellite resource cost of the CSTRS scheme reduces significantly, since more CAVs can be served by RSUs by adaptively adjusting SSGs. However, *fixed-number SSG* strategies struggle to effectively manage resources across satellite and terrestrial networks in dynamic environments. In this case, despite increased RSU densities, the sensing interval remains small for SSGs, resulting in a high resource cost.

Finally, we investigate the resource cost for CAVs in rural areas from the LEO satellite and terrestrial RSUs as shown in Fig. 9. We can observe that the resource cost from the LEO satellite decreases for CAVs with increasing RSU density in rural areas, while the resource cost from RSUs increases to serve more CAVs. Specifically, the decline in satellite resource cost is more pronounced than the increase in RSU resource cost since the unit cost of satellite resources is higher than that of RSU resources. In this case, cooperative resource scheduling from satellite and terrestrial networks can effectively reduce the overall resource cost with more network support from RSUs.

VIII. Conclusion

In this article, we have investigated a joint communication and computing resource scheduling problem for infrastructure-assisted environment sensing in STVN. To cope with the dynamic network environment and satisfy the stringent freshness and reliability requirements for environment sensing, we have proposed the CSTRS scheme, which is a hybrid data-model co-driven approach for resource scheduling in STVN to jointly find the optimal CAV partition, sensing interval, and resource allocation decisions. The proposed scheme can cooperatively manage resources from both satellite and terrestrial networks, capable of leveraging the advantages of different networks, thus reducing resource costs while satisfying service requirements in STVN. In the future, we will further investigate the resource scheduling strategy for multifarious vehicular services by managing resources from terrestrial networks and different satellites across constellations.

Appendix
Proof of Proposition 1

For each CAV, to satisfy the sensing result freshness requirement T^{th}, consecutive sensing data, either from the LEO satellite or connected RSUs, should be generated with an interval less than T^{th}. For the case when CAV u cannot consistently connect to RSUs throughout the entire time interval, ensuring the reliability requirement of environment sensing necessitates a satellite sensing interval of $T_u^S < T^{\text{th}}$. This guarantees the continuous reception of sensing results for the CAV. The sensing offset can be any time less than the sensing interval T_u^S. If CAV u can consistently connect to both the LEO satellite and RSUs during the time interval, there are three cases. The first two cases indicate that the freshness requirement can be satisfied through sensing from one source, either the LEO satellite or RSUs for an individual CAV. In these cases, either the sensing interval from the LEO satellite or RSUs should be less than T^{th}. For the third case, if the environment sensing requirement cannot be met with a single sensing source, then both the satellite and RSUs should be involved for environment sensing, and the following relation should be satisfied:

$$\frac{1}{T_u^S} + \frac{1}{T_u^T} > \frac{1}{T^{\text{th}}} \text{ and } T_u^S, T_u^T \in [T^{\text{th}}, 2T^{\text{th}}). \tag{31}$$

However, (31) serves as a necessary but not sufficient condition for ensuring the sensing freshness requirement. To avoid potentially outdated sensing results, a proper satellite sensing time offset ψ_u^S should be determined. Let jT_u^T and $kT_u^S + \psi_u^S$ denote the time stamps of the jth RSU sensing and kth satellite sensing, respectively. To satisfy the freshness requirement, the sensing time stamp of the satellite should not fall within any of the following ranges.

1) $kT_u^S + \psi_u^S \in [jT_u^T, (j+1)T_u^T - T^{\text{th}}]$: This indicates that after receiving the kth satellite sensing result, CAV u's sensing result become outdated before the $(j+1)$th RSU sensing starts.
2) $kT_u^S + \psi_u^S \in [jT_u^T + T^{\text{th}}, (j+1)T_u^T]$: This represents that after receiving jth RSU sensing result, CAV u's sensing result will be outdated before the kth satellite sensing starts.
3) $kT_u^S + \psi_u^S \in [(j+1)T_u^T - T_u^S, jT_u^T]$: This implies that the kth satellite sensing begins before the jth RSU sensing and the $k+1$th satellite sensing will begin after the $j+1$th RSU sensing. In other words, the jth RSU sensing result will be outdated since $T_u^T \geq T^{\text{th}}$.

Combining the above three cases, we can find that the freshness requirement cannot be satisfied if

$$\begin{aligned} &kT_u^S + \psi_u^S = jT_u^T + g, \ \exists j, k \in \mathbb{N} \\ &g \in \mathcal{L} = \left[0, T_u^T - T^{\text{th}}\right] \cup \left[T^{\text{th}}, T_u^T\right] \cup \left[T_u^T - T_u^S, 0\right] \end{aligned} \tag{32}$$

which can be rewritten as

$$jT_u^T - kT_u^S = \psi_u^S - g, \ \exists j, k \in \mathbb{N}. \tag{33}$$

According to the Bézout's identity [34], there exists values $j, k \in \mathbb{N}$ such that

$$|jT_u^T - kT_u^S| = G \tag{34}$$

where $G = \gcd(T_u^T, T_u^S)$ is the greatest common divisor of two values. In this case, (32) is satisfied indicating the violation of the freshness requirement if

$$\exists\left(\psi_u^S - g\right) \mod G = 0. \tag{35}$$

In addition, the relation of two sensing intervals has the following proposition.

Proposition 3: If two different sensing interval $T_u^S \neq T_u^T$, $|T_u^S - T_u^T| \geq G$.

Proof: According to the definition of the greatest common divisor, there exist integers a and b, so that

$$T_u^S = aG, T_u^T = bG \tag{36}$$

where a and b are the coprime integers. In this case, we have

$$|T_u^S - T_u^T| = |a - b||G|. \tag{37}$$

Since $a \neq b$, $|a - b| \geq 1$. Therefore, $|T_u^S - T_u^T| \geq G$. ■

To this end, we can divide the values of the sensing interval pair into the following three cases.

1) $T_u^S > T_u^T$: Consider one interval $[T_u^T - T_u^S, 0] \subset \mathcal{L}$ where the range is given by $T_u^S - T_u^T$. Since $T_u^S - T_u^T \geq G$ according to Proposition 3, regardless of the value of ψ_u^S, there exists $g \in \mathcal{L}$ to satisfy (35).
2) $T_u^S < T_u^T$: Consider the interval $[0, T_u^T - T^{\text{th}}] \cup [T^{\text{th}}, T_u^T] = \mathcal{L}$ where the range is given by $(T_u^T - T^{\text{th}} - 0) + (T_u^T - T^{\text{th}}) = 2(T_u^T - T^{\text{th}})$. Since $T_u^T - T_u^S \geq G$ and $T_u^T > T_u^S \geq T^{\text{th}}$, we can have $2(T_u^T - T^{\text{th}}) \geq G$. In this case, there exists $g \in \mathcal{L}$ to satisfy (35).
3) $T_u^S = T_u^T$: Consider that $[0, T_u^T - T^{\text{th}}] \cup [T^{\text{th}}, T_u^T] = \mathcal{L}$, similarly, the range of the intervals is given by $2(T_u^T - T^{\text{th}})$. Since $2T^{\text{th}} > T_u^T \geq T^{\text{th}}$, we can have $2(T_u^T - T^{\text{th}}) < T_u^T = T_u^S = G$. Therefore, there exist feasible offset values such that (35) cannot be satisfied, given by

$$\psi_u^S \in \hat{\psi}_u^S = \left\{l\kappa \mid l\kappa \in \left(T_u^T - T^{\text{th}}, T^{\text{th}}\right) \ \forall l \in \mathbb{N}\right\}. \tag{38}$$

REFERENCES

[1] Q. Chen, Y. Xie, S. Guo, J. Bai, and Q. Shu, "Sensing system of environmental perception technologies for driverless vehicle: A review of state of the art and challenges," *Sens. Actuat. A, Phys.*, vol. 319, Mar. 2021, Art. no. 112566.

[2] "C-V2X use cases volume II: Examples and service level requirements," 5GAA, Munich, Germany, White Paper, Aug. 2020.

[3] E. Arnold, M. Dianati, R. de Temple, and S. Fallah, "Cooperative perception for 3D object detection in driving scenarios using infrastructure sensors," *IEEE Trans. Intell. Transp. Syst.*, vol. 23, no. 3, pp. 1852–1864, Mar. 2022.

[4] X. Liu, T. Ma, Z. Tang, X. Qin, H. Zhou, and X. Shen, "UltraStar: A lightweight simulator of ultra-dense LEO satellite constellation networking for 6G," *IEEE/CAA J. Autom. Sinica*, vol. 10, no. 3, pp. 632–645, Mar. 2023.

[5] H. Wu, M. He, X. Shen, W. Zhuang, N. Dao, and W. Shi, "Network performance analysis of satellite-terrestrial vehicular network," *IEEE Internet Things J.*, vol. 11, no. 9, pp. 16829–16844, May 2024.

[6] A. Van Etten, "Satellite imagery multiscale rapid detection with windowed networks," in *Proc. IEEE WACV*, 2019, pp. 735–743.

[7] X. Zhu, C. Jiang, L. Yin, L. Kuang, N. Ge, and J. Lu, "Cooperative multigroup multicast transmission in integrated terrestrial-satellite networks," *IEEE J. Sel. Areas Commun.*, vol. 36, no. 5, pp. 981–992, May 2018.

[8] H. Wu, J. Chen, C. Zhou, J. Li, and X. Shen, "Learning-based joint resource slicing and scheduling in space-terrestrial integrated vehicular networks," *J. Commun. Inf. Nets.*, vol. 6, no. 3, pp. 208–223, Sep. 2021.

[9] C. Zhou, H. Wu, M. He, W. Wu, N. Cheng, and X. Shen, "Adaptive access mode selection in space-ground integrated vehicular networks," in *Proc. IEEE GLOBECOM*, 2021, pp. 1–6.

[10] J. Chu and X. Chen, "Robust design for integrated satellite-terrestrial Internet of Things," *IEEE Internet Things J.*, vol. 8, no. 11, pp. 9072–9083, Jun. 2021.

[11] Y.-C. Liang, J. Tan, H. Jia, J. Zhang, and L. Zhao, "Realizing intelligent spectrum management for integrated satellite and terrestrial networks," *J. Commun. Inf. Netw.*, vol. 6, no. 1, pp. 32–43, Mar. 2021.

[12] Z. Gao, A. Liu, C. Han, and X. Liang, "Non-orthogonal multiple access based average age of information minimization in LEO satellite-terrestrial integrated networks," *IEEE Trans. Green Commun. Netw.*, vol. 6, no. 3, pp. 1793–1805, Sep. 2022.

[13] X. Zhang, D. Guo, K. An, G. Zheng, S. Chatzinotas, and B. Zhang, "Auction-based multichannel cooperative spectrum sharing in hybrid satellite-terrestrial IoT networks," *IEEE Internet Things J.*, vol. 8, no. 8, pp. 7009–7023, Apr. 2021.

[14] M. He, C. Zhou, H. Wu, and X. Shen, "Learning-based cache placement and content delivery for satellite-terrestrial integrated networks," in *Proc. IEEE GLOBECOM*, 2021, pp. 1–6.

[15] X. Zhang et al., "Cost-effective hybrid computation offloading in satellite-terrestrial integrated networks," *IEEE Internet Things J.*, vol. 11, no. 22, pp. 36786–36800, Nov. 2024.

[16] D. Han et al., "Two-timescale learning-based task offloading for remote IoT in integrated satellite-terrestrial networks," *IEEE Internet Things J.*, vol. 10, no. 12, pp. 10131–10145, Jun. 2023.

[17] L. Chen et al., "Time-varying resource graph based processing on the way for space-terrestrial integrated vehicle networks," *IEEE Trans. Mobile Comput.*, vol. 23, no. 2, pp. 1985–2002, Feb. 2024.

[18] "Study on architecture aspects for using satellite access in 5G; (Release 17), Version 17.2.0," 3GPP, Sophia Antipolis, France, Rep. 23.737, 2021.

[19] S. Kaul, R. Yates, and M. Gruteser, "Real-time status: How often should one update?" in *Proc. IEEE INFOCOM*, 2012, pp. 2731–2735.

[20] "Intelligent transport systems (ITS); vehicular communications; basic set of applications; part 2: Specification of cooperative awareness basic service," ETSI, Sophia Antipolis, France, TR 302 637-2, 2019.

[21] H. Teng, Z. Li, K. Cao, S. Long, S. Guo, and A. Liu, "Game theoretical task offloading for profit maximization in mobile edge computing," *IEEE Trans. Mobile Comput.*, vol. 22, no. 9, pp. 5313–5329, Sep. 2023.

[22] N. Ramakrishnan and T. Soni, "Network traffic prediction using recurrent neural networks," in *Proc. IEEE ICMLA*, 2018, pp. 187–193.

[23] Y. Zhang, S. Wang, B. Chen, J. Cao, and Z. Huang, "TrafficGAN: Network-scale deep traffic prediction with generative adversarial nets," *IEEE Trans. Intell. Transp. Syst.*, vol. 22, no. 1, pp. 219–230, Jan. 2021.

[24] M. Cygan, Ł. Kowalik, and M. Wykurz, "Exponential-time approximation of weighted set cover," *Inf. Process. Lett.*, vol. 109, no. 16, pp. 957–961, 2009.

[25] M. Clerc and J. Kennedy, "The particle swarm-explosion, stability, and convergence in a multidimensional complex space," *IEEE Trans. Evol. Comput.*, vol. 6, no. 1, pp. 58–73, Feb. 2002.

[26] W. Saad, Z. Han, M. Debbah, A. Hjorungnes, and T. Basar, "Coalitional game theory for communication networks," *IEEE Signal Process. Mag.*, vol. 26, no. 5, pp. 77–97, Sep. 2009.

[27] A. Bogomolnaia and M. O. Jackson, "The stability of hedonic coalition structures," *Games Econ. Behav.*, vol. 38, no. 2, pp. 201–230, 2002.

[28] M. J. Neely, *Stochastic Network Optimization With Application to Communication and Queueing Systems* (Synthesis Lectures on Learning, Networks, and Algorithms), vol. 3. Cham, Switzerland: Springer, 2010.

[29] J. Schulman, F. Wolski, P. Dhariwal, A. Radford, and O. Klimov, "Proximal policy optimization algorithms," 2017, *arXiv:1707.06347*.

[30] I. Leyva-Mayorga et al., "Non-geostationary orbit constellation design for global connectivity," in *Non-Geostationary Satellite Communications Systems*. London, U.K.: IET, 2023, pp. 237–267.

[31] T. T. de Almeida, L. de Carvalho Gomes, F. M. Ortiz, J. G. R. Júnior, and L. H. M. Costa, "Comparative analysis of a vehicular safety application in NS-3 and veins," *IEEE Trans. Intell. Transp. Syst.*, vol. 23, no. 1, pp. 620–629, Jan. 2022.

[32] K. Tan, L. Feng, G. Dán, and M. Törngren, "Decentralized convex optimization for joint task offloading and resource allocation of vehicular edge computing systems," *IEEE Trans. Veh. Technol.*, vol. 71, no. 12, pp. 13226–13241, Dec. 2022.

[33] L. F. Bittencourt, J. Diaz-Montes, R. Buyya, O. F. Rana, and M. Parashar, "Mobility-aware application scheduling in fog computing," *IEEE Cloud Comput.*, vol. 4, no. 2, pp. 26–35, Mar. 2017.

[34] G. A. Jones and J. M. Jones, *Elementary Number Theory*. London, U.K.: Springer-Verlag, 1998.

Mingcheng He (Graduate Student Member, IEEE) received the B.Sc. and M.Eng. degrees from Shanghai Jiao Tong University, Shanghai, China, in 2017 and 2020, respectively. He is currently pursuing the Ph.D. degree with the Department of Electrical and Computer Engineering, University of Waterloo, Waterloo, ON, Canada.

His research interests include network slicing in satellite-terrestrial integrated networks and artificial intelligence for future wireless networks.

Huaqing Wu (Member, IEEE) received the B.E. and M.E. degrees from Beijing University of Posts and Telecommunications, Beijing, China, in 2014 and 2017, respectively, and the Ph.D. degree from the University of Waterloo, Waterloo, ON, Canada, in 2021.

She is currently an Assistant Professor with the Department of Electrical and Software Engineering, University of Calgary, Calgary, AB, Canada. She was as a Postdoctoral Fellow with the Department of Electrical and Computer Engineering, McMaster University, Hamilton, ON, from 2021 to 2022. Her current research interests include B5G/6G, space-air-ground integrated networks, Internet of vehicles, mobile/edge computing/caching, and artificial intelligence for future networking.

Dr. Wu received the Best Paper Awards at IEEE GLOBECOM 2018, the Chinese Journal on Internet of Things 2020 and the IEEE GLOBECOM 2022, and the prestigious Natural Sciences and Engineering Research Council of Canada Postdoctoral Fellowship Award in 2021. She serves as an Associate Editor for IEEE COMMUNICATIONS SURVEYS AND TUTORIALS since 2024, IEEE NETWORK since 2023, and *Security and Safety Journal* since 2021.

Xuemin (Sherman) Shen (Fellow, IEEE) received the Ph.D. degree in electrical engineering from Rutgers University, New Brunswick, NJ, USA, in 1990.

He is a University Professor with the Department of Electrical and Computer Engineering, University of Waterloo, Waterloo, ON, Canada. His research interests include network resource management, wireless network security, Internet of Things, AI for networks, and vehicular networks.

Dr. Shen received the West Lake Friendship Award from Zhejiang Province in 2023, the President's Excellence in Research from the University of Waterloo in 2022, the Canadian Award for Telecommunications Research from the Canadian Society of Information Theory in 2021, the R.A. Fessenden Award in 2019 from IEEE, Canada, the Award of Merit from the Federation of Chinese Canadian Professionals (Ontario) in 2019, the James Evans Avant Garde Award in 2018 from the IEEE Vehicular Technology Society, the Joseph LoCicero Award in 2015, the Education Award in 2017 from the IEEE Communications Society (ComSoc), the Technical Recognition Award from the Wireless Communications Technical Committee in 2019 and the AHSN Technical Committee in 2013, the Excellent Graduate Supervision Award in 2006 from the University of Waterloo, and the Premier's Research Excellence Award in 2003 from the Province of Ontario, Canada. He is the Past President of the IEEE Communications Society. He was the Vice President of the Technical and Educational Activities, the Vice President of the Publications, the Member-at-Large on the Board of Governors, the Chair of the Distinguished Lecturer Selection Committee, and a Member of the IEEE Fellow Selection Committee of the ComSoc. He served as the Editor-in-Chief for IEEE INTERNET OF THINGS JOURNAL, IEEE NETWORK, and *IET Communications*. He is a registered Professional Engineer of Ontario, a Foreign Member of the Chinese Academy of Engineering, an International Fellow of the Engineering Academy of Japan, a Distinguished Lecturer of the IEEE Vehicular Technology Society and Communications Society, and a Fellow of the Engineering Institute of Canada, the Canadian Academy of Engineering, and the Royal Society of Canada.

Weihua Zhuang (Fellow, IEEE) received the B.Sc. and M.Sc. degrees in electrical engineering from Dalian Maritime University, Dalian, China, and the Ph.D. degree in electrical engineering from the University of New Brunswick, Fredericton, NB, Canada.

Since 1993, she has been a Faculty Member with the Department of Electrical and Computer Engineering, University of Waterloo, Waterloo, ON, Canada, where she is a University Professor and a University Research Chair of Wireless Communication Networks. Her current research interests include network architecture, algorithms and protocols, and service provisioning in future communication systems.

Dr. Zhuang is the recipient of the Women's Distinguished Career Award in 2021 from the IEEE Vehicular Technology Society, the R.A. Fessenden Award in 2021 from IEEE Canada, the Award of Merit in 2021 from the Federation of Chinese Canadian Professionals in Ontario, and the Technical Recognition Award in Ad Hoc and Sensor Networks in 2017 from the IEEE Communications Society. She is the President and an Elected Member of the Board of Governors of the IEEE Vehicular Technology Society. She was the Editor-in-Chief of IEEE TRANSACTIONS ON VEHICULAR TECHNOLOGY from 2007 to 2013, an Editor of IEEE TRANSACTIONS ON WIRELESS COMMUNICATIONS from 2005 to 2009, the General Co-Chair of IEEE/CIC International Conference on Communications, China, in 2021, the Technical Program Committee Chair/Co-Chair of IEEE Vehicular Technology Conference Fall 2016 and Fall 2017, the TPC Symposia Chair of the IEEE Globecom 2011, and an IEEE Communications Society Distinguished Lecturer from 2008 to 2011. She is a Fellow of the Royal Society of Canada, the Canadian Academy of Engineering, and the Engineering Institute of Canada.